applied sciences

MDPI

Article

Optimization of Process Parameters for Turning Hastelloy X under Different Machining Environments Using Evolutionary Algorithms: A Comparative Study

Vinothkumar Sivalingam [1], Jie Sun [1], Siva Kumar Mahalingam [2], Lenin Nagarajan [2,*], Yuvaraj Natarajan [2], Sachin Salunkhe [2], Emad Abouel Nasr [3], J. Paulo Davim [4] and Hussein Mohammed Abdel Moneam Hussein [5,6]

1 Key Laboratory of High-Efficiency and Clean Mechanical Manufacture, National Demonstration Center for Experimental Mechanical Engineering Education, School of Mechanical Engineering, Shandong University, Jinan 250061, China; svkceg@gmail.com (V.S.); sunjie@sdu.edu.cn (J.S.)
2 Department of Mechanical Engineering, Vel Tech Rangarajan Dr. Sagunthala R&D Institute of Science and Technology, Chennai 600 062, Tamilnadu, India; lawan.sisa@gmail.com (S.K.M.); drnyuvaraj@veltech.edu.in (Y.N.); drsalunkesachin@veltech.edu.in (S.S.)
3 Industrial Engineering Department, College of Engineering, King Saud University, Riyadh 11421, Saudi Arabia; eabdelghany@ksu.edu.sa
4 Department of Mechanical Engineering, Campus Universitário de Santiago, University of Aveiro, 3810-193 Aveiro, Portugal; pdavim@ua.pt
5 Department of Mechanical Engineering, Faculty of Engineering, Helwan University, Cairo 11732, Egypt; hussein@h-eng.helwan.edu.eg
6 Department of Mechanical Engineering, Faculty of Engineering, Ahram Canadian University, 6th of October City 19228, Egypt
* Correspondence: n.lenin@gmail.com; Tel.: +91-9976909647

Citation: Sivalingam, V.; Sun, J.; Mahalingam, S.K.; Nagarajan, L.; Natarajan, Y.; Salunkhe, S.; Nasr, E.A.; Davim, P.; Hussein, H.M.A.M. Optimization of Process Parameters for Turning Hastelloy X under Different Machining Environments Using Evolutionary Algorithms: A Comparative Study. *Appl. Sci.* **2021**, *11*, 9725. https://doi.org/10.3390/app11209725

Academic Editor: Vladimir Modrak

Received: 6 September 2021
Accepted: 11 October 2021
Published: 18 October 2021

Abstract: In this research work, the machinability of turning Hastelloy X with a PVD Ti-Al-N coated insert tool in dry, wet, and cryogenic machining environments is investigated. The machinability indices namely cutting force (CF), surface roughness (SR), and cutting temperature (CT) are studied for the different set of input process parameters such as cutting speed, feed rate, and machining environment, through the experiments conducted as per L_{27} orthogonal array. Minitab 17 is used to create quadratic Multiple Linear Regression Models (MLRM) based on the association between turning parameters and machineability indices. The Moth-Flame Optimization (MFO) algorithm is proposed in this work to identify the optimal set of turning parameters through the MLRM models, in view of minimizing the machinability indices. Three case studies by considering individual machinability indices, a combination of dual indices, and a combination of all three indices, are performed. The suggested MFO algorithm's effectiveness is evaluated in comparison to the findings of Genetic, Grass-Hooper, Grey-Wolf, and Particle Swarm Optimization algorithms. From the results, it is identified that the MFO algorithm outperformed the others. In addition, a confirmation experiment is conducted to verify the results of the MFO algorithm's optimal combination of turning parameters.

Keywords: Hastelloy X; turning; cutting force; surface roughness; liquid nitrogen; grass-hooper optimization algorithm; moth-flame optimization algorithm

1. Introduction

Nickel-based (Ni) alloys attract more researchers nowadays for their broader applications in the fields like aerospace, automobile, biomedical, and allied industries. Hastelloy is one of the Ni-based alloys, and it holds few unique characteristics like good strength-to-weight ratio, resistance to corrosion, higher melting temperature, good toughness, etc. [1]. Mainly, Hastelloy X is used to fabricate the combustion chamber of an aircraft engine because of its high heat-resisting property. However, the holding of all the above-said properties by Hastelloy X, resulting in very poor machinability. In this sense, the manufacturing industries face a difficult task in improving Hastelloy X machinability using traditional machining methods. [2]. Furthermore, the reduction of cutting forces (CF), surface roughness (SR), and cutting temperature (CT) during Hastelloy X machining adds to the difficulty of achieving good machinability. As a result, several researchers have worked on various research projects over time to increase the machinability of Hastelloy. Furthermore, they performed these tests under dry, wet, and cryogenic cooling conditions in order to demonstrate an increase in machinability. Therefore, these literatures are critically reviewed, and the extracted information is given here for ready reference to the readers.

Kadirgama et al. [3] studied the impact on cutting force by the parameters, namely axial depth, cutting speed, and feed rate while milling Hastelloy C-22HS. The models using Response Surface Methodology were developed using experimentation and Finite Element Analysis to predict the optimized cutting force. Kadirgama et al. [4] investigated the tool behavior such as tool wear and tool life during machining of Hastelloy C-22HS under wet conditions. PVD and CVD multilayer coated carbide tools were used for machining. The tool life was decreased in all the cases while increasing the cutting parameters, namely cutting speed (v_c), feed rate *(f)*, and axial depth (a_p). Altin [2] studied the machinability of Ni-based (Hastelloy X) alloy under dry cutting conditions. The CF and SR were analyzed against the multilayer coated insert and various v_c. The experimentation results showed that the abrasiveness of the carbide particles on the tool and the mechanical loading had a growing influence on the CF. Sofuoğlu et al. [5] studied the impact of the v_c, tool extended length, and novel methods, namely Conventional Turning (CT), Ultrasonic Assisted Turning (UAT) and Hot-Ultrasonic Assisted Turning (HUAT) on the SR, a_p, and CT while machining Hastelloy X. The reduction in SR and increment in regular a_p and CT were attained in UAT and HUAT compared to CT. Dhananchezian [6] conducted the machinability study on Hastelloy C-276 under dry and cryogenic liquid nitrogen (LN_2) cooling conditions using turning operation. The output responses such as CT, CF, SR, chip morphology, and tool wear under dry turning were compared with LN_2 cooling-based turning. A considerable reduction in all the output responses was noted under liquid nitrogen cooling-based turning.

Kesavan et al. [7] conducted the CNC turning of Hastelloy C276 by varying v_c and the fixed values of *f*, a_p. The experimentation was executed under dry and LN_2 conditions. Further, Deform 3D analytical tool was used to create the simulation model based on the experimental design to identify the optimal cutting conditions. From the experimentation and simulated model results, it was evident that the cutting temperate and machining forces have been significantly reduced while machining under cryogenic cooling conditions rather than dry conditions. Dhananchezian and Rajkumar [8] examined the SR and Tool Wear characteristics of Nimonic 90 alloy and Hastelloy C-276 dry turning. During the turning process, various cutting inserts were used. In both cases, the roughness and tool wear metrics were observed to be larger as the turning length was increased. Dhananchezian and Rajkumar [8] made a comparative analysis on the tool wear rate and SR during the turning of Hastelloy C-22 underneath dry and LN_2 cooling conditions. A substantial drop in the SR was found in the turning of Hastelloy under LN_2 cooling rather than dry turning.

Oschelski et al. [9] used the Box-Behnken method to design the experiments by considering the ranges of parameters, namely v_c, a_p, lubricating conditions, constant *f*, and (wet, dry, and reduced quantity lubrication) for finish turning the Hastelloy X. The experimental results showed that the v_c, a_p, and interactions were the most significant factors affecting the SR. Next, Venkatesan et al. [10] reported the machinability study on Hastelloy X with PVD and CVD coated tools in comparison with dry and Minimum Quantity Lubrication (MQL) conditions. A mixture of coconut oil with Hexagonal Boron Nitride (HBN) nanoparticles was used as nanofluid for lubrication. Significant reductions in CF, SR, and tool wear were observed in MQL-PVD combination than MQL-CVD and dry-PVD. Finally, Sivalingam et al. [11] investigated the influence of whisker-reinforced ceramic tools on tool wear, SR, and tool chattering under dry and Atomization-based Cutting Fluid (ACF) cooling conditions when turning Inconel 718 material. Investigation results stated that the flank wear and SR of the tool were significantly reduced under ACF cooling conditions due to limited notching and fracture of the tool edge at the tool-chip interface.

Zhao et al. [12] investigated the characteristics of chip formation when machining NiTi shape memory alloys under different v_c with constant f, a_p. The shape of the chip and microstructure were examined to expose the chip flow behavior. The martensitic phase transformation seemed to have a noticeable effect on the material flow behavior and indeed on the chip formation. [11] investigated the possibility of improving the machinability of Inconel 718 alloy under a dry and atomized spray cutting fluid system. The turning of Inconel 718 alloy with ceramic inserts was carried out by varying the cutting parameters. The output responses such as tool wear, power consumption, surface topography, machine vibrations, chip morphology, and machining cost were analyzed against the experimental design of input parameters. It was observed that the atomized spray cutting fluid technique yielded better results than dry machining.

The effect of LN_2 cooling in improving the machinability of Hastelloy X is discussed in the following literature. Chetan et al. [13] investigated the turning of Nimonic 90 alloy using uncoated tungsten carbide inserts under the modes like dry, MQL, and cryogenic cutting. At lower v_c, the cutting performance of the cryogenically treated tool was good than the untreated tool. But, the performance of the tool under MQL and LN_2 was good in terms of minimum tool wear at a higher cutting speed. Further, a good SR was obtained under dry and MQL modes than LN_2 cooling mode at all levels of cutting speed. Iturbe et al. [14] compared the effects of liquid nitrogen and MQL based cryogenic cooling with conventional cooling. For short machining times, the cryogenic cum MQL cooling outperformed conventional cooling.

Sivaiah and Chakradhar [15] compared the results of LN_2 machining like tool wear, feed force, CF and CT, chip characteristics, and SR with the wet condition during machining of heat-treated 17-4 Precipitation Hardenable Stainless Steel. The LN_2 machining outperformed even at high f to reduce all the above-said parameters compared with wet machining. Tebaldo et al. [16] studied the machinability of Inconel 718 under different machining conditions and lubricating systems. The highest wear resistance was obtained while using the CVD-coated tools under conventional lubricated conditions. But, the MQL system provided good lubrication than cooling with lesser cost and low environmental impact. Shokrani et al. [17] investigated the impact of using different cooling systems, namely MQL, cryogenic and hybrid of cryogenic and MQL, during the CNC milling of Inconel 718 alloy material. Comparatively, the hybrid cooling system yielded better results in terms of good machinability, less SR, and greater tool life. Mehta et al. [18] studied the parameters such as SR, CF, and tool wear during machining of Inconel 718 material. During machining, various sustainable environments, namely dry state, MQL, LN_2 cooling, hybridization of cold air and MQL, and hybridization of MQL and LN_2, were used. The input parameters such as a_p, f, and v_c were kept constant during machining under all the above-said environments. Better surface finish and minimum cutting force were observed during the cold air and MQL environment. Alternatively, the very least tool wear was observed under MQL and LN_2 hybrid cutting environment than the dry environment.

Further, the researchers had used different optimization tools to identify the suitable process parameter values for minimizing the manufacturer's objectives. A few of them are discussed here. Khalilpourazari and Khalilpourazary [19] proposed an algorithm, namely Robust Grey Wolf Optimizer (RGWO), to minimize total production time by identifying the optimal input parameters multi-pass milling process. The parameter tuning during optimization was carried out using the Taguchi method. Further, an efficient constraint handling approach was implemented to handle the complex constraints of the problem.

The results concluded that the RGWO outperformed the meta-heuristic algorithms such as the multi-verse optimizer and dragonfly algorithm and the other solution methods in the literature. Khalilpourazari and Khalilpourazary [20] developed the lexicographic weighted Tchebycheff method to obtain the optimal decision parameters of the grinding process for maximizing the quality of the surface and production rate and minimizing the machining time and cost. GAMS software was used for this purpose. Khalilpourazari and Khalilpourazary [21] used a novel strategy, namely Robust Stochastic Novel Search, to identify the optimal values of the grinding process parameters to minimize process cost and to maximize the rate of production and surface quality. The proposed method outperformed previously proposed methodologies and novel algorithms, including Multi-Population Ensemble Differential Evolution and Heterogeneous Comprehensive Learning Particle Swarm Optimization.

Rao et al. [22] optimized the abrasive water-jet machining parameters to minimize the kerf and surface roughness using the Jaya algorithm and the multi-objective Jaya algorithm. Better results were obtained through the used algorithms than the simulated annealing, particle swarm optimization, firefly algorithm, cuckoo search algorithm, blackhole algorithm, and biogeography-based optimization algorithms. Further, the PROMETHEE method was used to handpick a specific solution among the possible Pareto-optimal solutions obtained through the proposed algorithms based on the given requirements. Rao et al. [23] obtained the optimal set of process parameters of focused ion beam micro-milling, laser cutting, wire-electric discharge machining, and electrochemical machining processes. The maximization of material removal rate and minimization of SR were considered as the objectives in all the processes. The multi-objective Jaya algorithm was implemented to find the optimal solutions in all the cases. The test results showed that the implemented algorithms produced good results compared to other algorithms such as Genetic Algorithm, Non-dominated Sorting Genetic Algorithm, iterative search, and biogeography-based optimization algorithm, Khalilpourazari and Khalilpourazary [24] carried out the optimization of grinding process parameters to improve the SR and reduce production cost and time. A multi-objective dragonfly algorithm was employed for optimizing the process parameters. Results revealed that the proposed algorithm outperformed the Non-dominated Sorting Genetic Algorithm-II. Khalilpourazari and Khalilpourazary [25] proposed a novel hybrid algorithm, Sine–Cosine Whale Optimization Algorithm, to optimize the process parameters of the multi-pass milling process by minimizing the total production time. Almeida et al. [26] optimized the variable-angle composite cylinders via filament winding manufacturing process using GA. Similarly, Wang et al. [27] proposed a reliability-based design optimization technique to improve the buckling load of winding cylinders subjected to radial compression. The moving search windows in the Kriging metamodel are used to accelerate its convergence and reduce the number of training iterations. The results of this study demonstrated the advantages of adopting a variable stiffness design for achieving a maximum load capacity. Almeida et al. [28] proposed a genetic algorithm (GA) to enhance the strength of a cylindrical shell under internal pressure by optimizing the stacking sequence. The results offered asymmetric and non-conventional angles for internally pressured composite tubes, as opposed to the well-known ± 55° winding angle advice (for first ply failure approach).

In this research work, turning experiments are conducted on the Hastelloy X material using the PVD TiAlN carbide insert tool under dry, wet, and LN_2 environments. The v_c, f, a_p, and machining environment are considered input turning process parameters, and CF, SR, and CT are considered machinability indices. The evolutionary algorithms namely grasshopper optimization (GHO) [29–31], genetic algorithm (GA) [32–34], particle swarm optimization (PSO) [35,36], moth flame (MFO) [37,38], grey wolf optimization (GWO) [39–41] algorithms are used to identify the optimal set of turning process parameters (MATLAB R2020b version). A clear picture of the experimentation and subsequent processes are detailed in Figure 1.

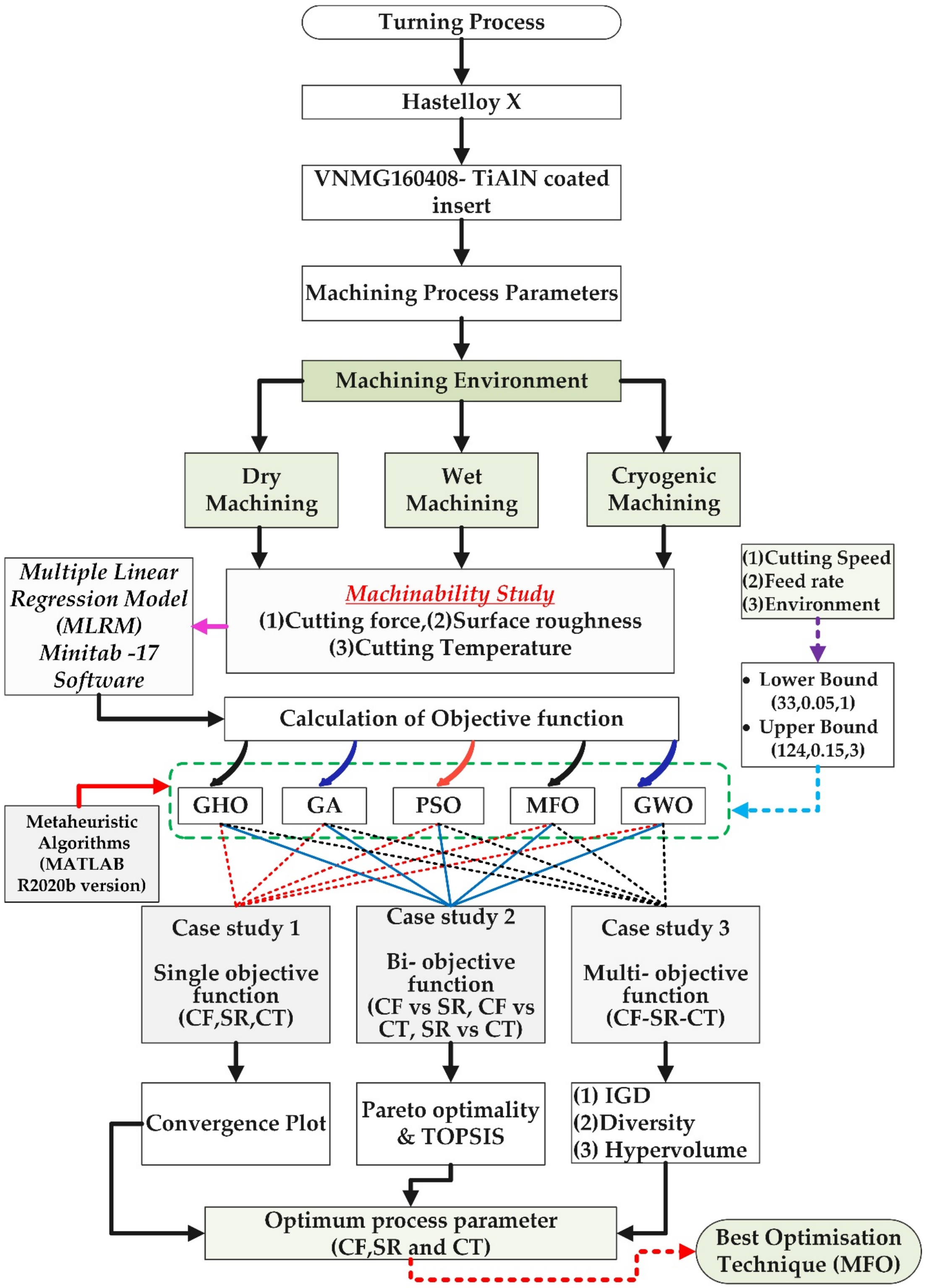

Figure 1. Flow chart of experimental part and metaheuristic algorithm.

2. Experimentation Details

The Hastelloy X bar having 20 mm diameter and 300 mm length is used for conducting the turning experiments on a C6140H turning machine. VNMG160408-SM1105 PVD TiAlN cutting tool inserts are used to do the turning operation. The impact of tool wear on the machinability indices is completely eliminated by using new inserts every time. The CF (Tangential Force, F_z) is calculated with a 9257B Kistler dynamometer, and the value is manipulated with dynoware software. The workpiece surface roughness (Ra) is measured using a contact-type surface roughness tester (TR200), a cutoff length of 0.8 mm, and a traverse length of 4 mm. For measuring the CT, a FORTIC 226 infrared imaging sensor is used. Cryogenic equipment consists of a self-pressurized pump, cryogenic dewar tank capacity of 50 L. At a pressure of 0.3 bar, LN_2 was sprayed onto the work-tool interface using a copper nozzle diameter of 3mm. Figure 2 depicts a schematic representation of the experimental setup. The detailed experimental conditions are shown in Table 1.

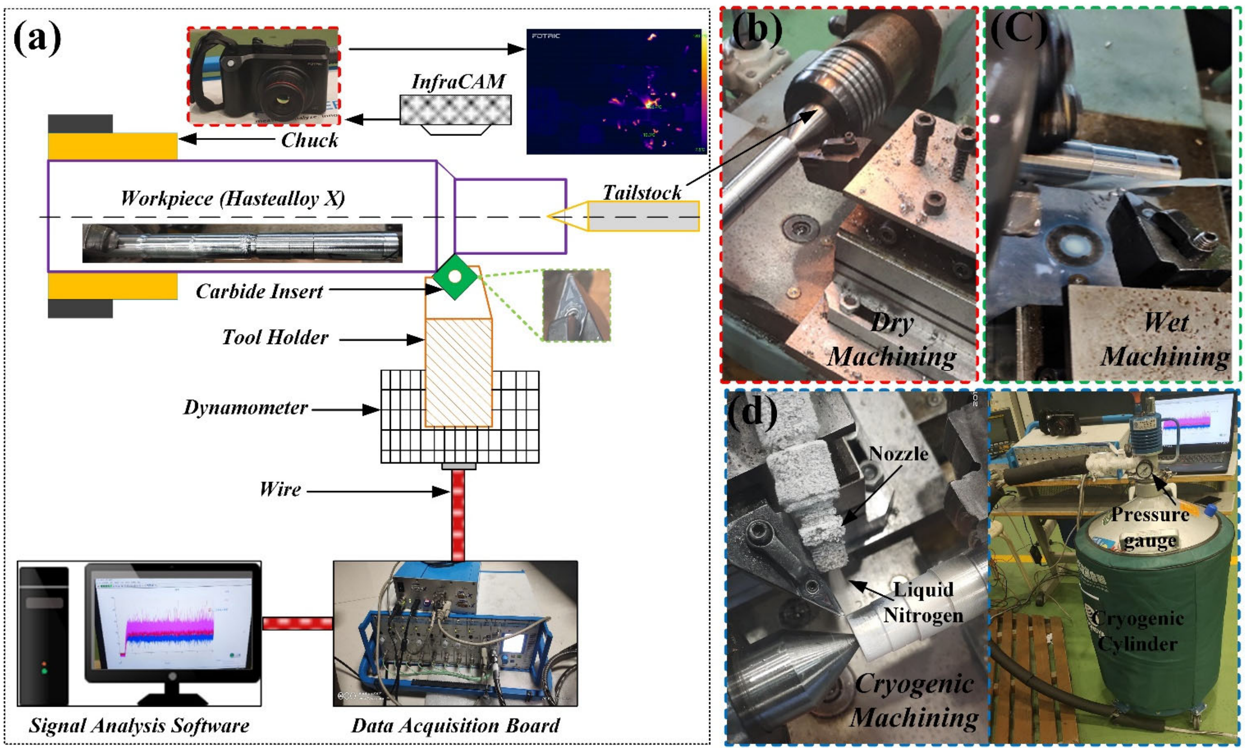

Figure 2. (**a**) Schematic View, Experimental Setup (**b**) Dry (**c**) Wet (**d**) Cryogenic Machining.

Table 1. Experimental Conditions.

Items	Descriptions
Workpiece	Hastealloy × (Ø20 × 300 mm)
Material Properties	**Chemical Composition (%):** Ni:50, Cr:21, Mo:17, Fe:2, Co:1,W:1, Mn:0.80, Al:0.05, Si:0.08, C:0.01, B:0.01 **Physical Properties:** Tensile strength:1370 MPa, Yield Strength: 1170 Mpa, Hardness:388 HB
Insert Specification	VNMG160408-SM1105, PVD TiAlN coated carbide insert, Sandvick
Nose radius	0.8 mm
Rake and relief angle	7°, 6°
Depth of cut (a_P)	0.1 mm
Length of cut (Loc)	60 mm
Environment	Dry, Wet and Cryogenic machining
Cutting Fluid	Vegetable-based oil
Cutting force	Kistler 9257B dynamometer Cutting
Cutting temperature	FORTIC 226 infrared radiation imaging sensor
Surface Roughness	TR200 portable surface roughness tester Evaluation and sampling Lengths are 4 and 0.8 mm

In this work, turning experiments were performed using $L^3{}_{27}$ full factorial experimental design using Minitab 17. three factors are considered for this experiment: v_c, *f*, and environment; each factor has three different levels, as shown in Table 2.

Table 2. $L^3{}_{27}$ full factorial experimental design.

Factors	Unit	Symbol	Level 1	Level 2	Level 3
Cutting speed (v_c)	m/min	A	33	87	124
Feed rate (*f*)	mm/rev	B	0.05	0.1	0.15
Environment		C	1 **(Dry)**	2 **(Wet)**	3 **(Cryogenic)**

The experimental design and the corresponding measurement of machinability indices are presented in Table 3.

Table 3. Experimental design values.

S.no	Cutting Speed	Feed Rate	Environmen t	Cuting Force	Surface Roughness	Cutting Temperatur e
	m/min	mm/rev		Fz (N)	Ra (µm)	°C
1	33	0.05	Dry	256	3.42	380
2	87	0.05	Dry	192	3.01	416
3	124	0.05	Dry	165	2.98	472
4	33	0.1	Dry	339	2.96	435
5	87	0.1	Dry	281	2.83	477
6	124	0.1	Dry	220	2.72	515
7	33	0.15	Dry	430	2.75	510
8	87	0.15	Dry	385	2.62	550
9	124	0.15	Dry	322	2.53	596
10	33	0.05	Wet	245	3.25	250
11	87	0.05	Wet	186	2.86	313
12	124	0.05	Wet	156	2.80	347
13	33	0.1	Wet	302	2.87	386
14	87	0.1	Wet	276	2.74	414
15	124	0.1	Wet	208	2.68	472
16	33	0.15	Wet	412	2.69	491
17	87	0.15	Wet	368	2.53	515
18	124	0.15	Wet	308	2.43	565
19	33	0.05	Cryogeic	228	2.65	50
20	87	0.05	Cryogeic	168	2.48	95
21	124	0.05	Cryogeic	132	2.29	110
22	33	0.1	Cryogeic	275	2.2	90
23	87	0.1	Cryogeic	249	2.01	135
24	124	0.1	Cryogeic	168	1.96	140
25	33	0.15	Cryogeic	367	1.92	110
26	87	0.15	Cryogeic	320	1.84	130
27	124	0.15	Cryogeic	279	1.76	165

3. Results and Discussion

This section is divided into three case studies. Case study 1: Minimization of machinability indices individually; Case study 2: Simultaneous minimization of dual machinability indices by considering three combinations; Case study 3: Simultaneous minimization of all three indices. The quadratic Multiple Linear Regression Models (MLRM) are formulated for evaluating the minimum values of machinability indices in all the cases. The Moth-Flame Optimization (MFO) algorithm is proposed to identify the optimal set of turning process parameters in view of minimizing the objectives. The effectiveness of the proposed algorithm is tested against the results of other optimization algorithms such as Genetic Algorithm, Grass-Hooper Optimization (GHO), Grey-Wolf Optimization (GWO), and Particle Swarm Optimization (PSO). Pseudocode for optimization algorithms is shown in the Figure 3. The general parameters used in algorithms are the maximum population size: 50, and the maximum no. of iterations: 100 (MATLAB R2020b). Twenty-seven runs are executed for each algorithm in all the cases. The evaluated results from the case studies are discussed below.

3.1. Case Study 1

Cutting force analysis and its minimization plays a crucial role in machining operation and understanding the cutting phenomena of the work material in different environments (dry, wet, and LN_2 machining). Moreover, after machining, the work material must be superior in surface quality [33]. On the other hand, minimizing the machining zone's temperature is necessary to retain the cutting temperature as low as possible. In this case study, the MLRM for minimizing all the machinability indices is developed using Minitab 17. The developed MLRM are given in Equations (1)–(3).

Objective functions 1.

$$\begin{aligned} &\textit{Minimize Cutting} = 212.7 - 0.244A + 703B + 20C \\ &\textit{Force} \qquad - 0.00571A^2 + 6289B^2 - 8.11C^2 \\ &\qquad\qquad - 0.60AB + 0.053AC - 143BC \\ &R^2 = 0.98, Adj\,R^2 = 0.98 \end{aligned} \tag{1}$$

Objective functions 2.

$$\begin{aligned} &\textit{Minimize Surface} = 3.56 - 0.008A - 9.65B + 0.73C \\ &\textit{Roughness} \qquad + 0.000015A^2 + 19.3B^2 - 0.265C^2 \\ &\qquad\qquad + 0.023AB + 0.00028AC - 0.65BC \\ &R^2 = 0.98, Adj\,R^2 = 0.97 \end{aligned} \tag{2}$$

Objective functions 3.

$$\begin{aligned} &\textit{Minimize Cutting} = -0.083 + 0.076A + 2521B + 341.21C \\ &\textit{Temperature} \qquad + 0.0033A^2 - 1400B^2 - 118C^2 \\ &\qquad\qquad - 1.42AB - 0.16AC - 396.67BC \\ &R^2 = 0.97, Adj\,R^2 = 0.96 \end{aligned} \tag{3}$$

Three responses were considered in this section R1, R2 and R3, CF, SR and CT, respectively, as shown in Table 4.

Table 4. Minimization of machinability indices using evolutionary algorithms for Case study 1.

Algorithms	Cutting Speed (m/min)	Feed Rate (mm/rev)	Environment	Machinability Index Value	Iteration No.
			Cutting force		
MFO	124	0.05	3	127.10 N	2
GA	119.61	0.05	3	139.16 N	3
GHO	124	0.06	3	135.27 N	61
GWO	121.65	0.05	3	132.85 N	78
PSO	123.32	0.05	3	132.77 N	10
			Surface roughness		
MFO	124	0.05	3	1.78 μm	1
GA	86.23	0.147	3	1.88 μm	3
GHO	124	0.129	3	1.85 μm	39
GWO	134.17	0.15	3	1.81 μm	79
PSO	126.32	0.052	3	2.33 μm	10
			Cutting temperature		
MFO	34.04	0.05	3	33.19 °C	22
GA	80.77	0.05	3	78.98 °C	67
GHO	36	0.05	3	32.33 °C	65
GWO	39.57	0.06	3	48.44 °C	43
PSO	33.6	0.05	3	34.11 °C	26

Figure 4a present the convergence plot for cutting force using the evolutionary algorithms. It is observed that the response is converged in iteration no. 2 using the MFO algorithm. Provided the same response value is converged in iteration no. 3, 10, 61, and 78 based on GA, PSO, GHO, and GWO algorithms, respectively. Further, the response value is very minimum in the MFO algorithm and maximum in GA. The simplicity of the MFO algorithm along with the speed in searching is the prime reason for obtaining the best results in the present work. It is additionally inferred that the CF is very minimum in the LN_2 environment compared to the dry and wet machining environments. The LN_2 nozzle spray droplet acts as cushioning effect of the machining zone and, thus, minimizes the v_c [42].

Similarly, the convergence plots for the other two machinability indices are given in Figure 4b,c, respectively. The order of preferences of algorithms based on their performance in obtaining the minimum response values is MFO-GWO-GHO-GA-PSO for SR and MFO-GHO-PSO-GWO-GA for CT. Chattered vibrations are generally existing in the machining process, and this is significantly affecting the SR. The SR values are lower in the cryogenic machining than the dry and wet machining from the experimental value and predicted data.

Further, the cutting temperature is directly related to CF and SR. CT increases with an increase in v_c. The flow of cryogenic LN_2 (−196 °C) between tool and workpiece interface greatly reduces the CT in the machining zone compared with dry and wet machining[42].

(a) Moth-Flame Optimization Algorithm (MFO)

```
Initialize the parameters for Moth-flame
Initialize Moth position Mi randomly
For each i=1:n do
Calculate the fitness function fi
End For
While (iteration ≤ max_iteration) do
        Update the position of Mi
        Calculate the no. of flames
        Evaluate the fitness function fi
        If (iteration==1) then
                F = sort (M)
                OF = sort (OM)
Else
                F = sort (Mt-1, Mt)
                OF = sort (Mt-1, Mt)
End if
     For each i=1:n do
       For each j=1:d do
        Update the values of r and t
       Calculate the value of D w.r.t. corresponding Moth
       Update M(i,j) w.r.t. corresponding Moth
                End For
        End For
End While
Print the best solution
```

(b) Grass Hopper Optimization Algorithm (GHO)

```
Initialize the swarm Xi (i=1,2, 3,., n)
Initialize Cmax, Cmin and itemax
Calculate the fitness of each agent
T = the best search agent
While (I < itemax)
     update C
     For each search agent
         Normalize the distance between the
                 grasshoppers
          Update the position of current search agent
          Bring the current search agent back -
           -if it goes outside the boundaries
         End for
         Update T if there is a better solution
         I = I + 1
End While
Return
```

(c) Genetic Algorithm (GA)

```
{
Generation of initial population (Pi)
Evaluation of Pi
While (stopping criteria not satisfied) Repeat
          {
          For 1 to (no. of tournaments)
           {
             Select N chromosomes for tournament
             Find chromosome with lowest fitness
             Remove chromosome with lowest fitness
             Crossover (Creation of new chromosome)
              Evaluation of new chromosome
                    }
                    Mutation
                    Evaluation of mutated chromosome
          }
}
```

(d) Grey Wolf Optimization Algorithm (GWO)

```
Initialize no. of grey wolf (Xij – i =1,2,..nw and j=1,2,..nd)
While (it < nitr)
     Determine the fitness function Fik (k=1,2..nf) of each wolf
    Calculate Pareto optimal distance fi
    Sort fi in descending order and set as sfi and store the first
         wolf's data as Xit. and Fit.
    Using the sorted data, assign Xa. = X1, Xb. = X2. and Xd. = X3.
         Compute
         For each wolf
            Update the position using
              A1=2*a*rand()-a and C1 = 2*rand() and
                   Da.=abs(C1*Xa.-X i.) and X1. = Xa.-A1*Da.
              A2=2*a*rand()-a and C2 = 2*rand() and
                   Db.=abs(C1*Xb.-Xi.) and X2. = Xb.-A2*Db.
              A3=2*a*rand()-a and C3 = 2*rand() and
                   Dd.=abs(C1*Xd.-X i.) and X3. = Xd.-A3*Dd.
              X i. = (X1. + X2. + X3.)/3
              Check Xi. within bounds
         End
End
Using TOPSIS method convert Fit. into fi
Sort fi in descending order and display the first wolf's data
which is optimum data
```

(e) Particle Swarm Optimization Algorithm (PSO)

```
P = Particle Initialization ();
For i=1 to itrmax
       For each particle p in P do
            fp = f(p);
            If fp is better than f(pBest);
             pBest = p;
                  end
            end
        gBest = best p in P
        For each particle p in P do
        v = v + c1 *rand*(pBest – p) + C2 *rand*(gBest-P);
             p = p+v;
          end
end
```

Figure 3. Pseudocode for optimization algorithms (**a**) MFO (**b**) GHO (**c**) GA (**d**) GWO (**e**) PSO.

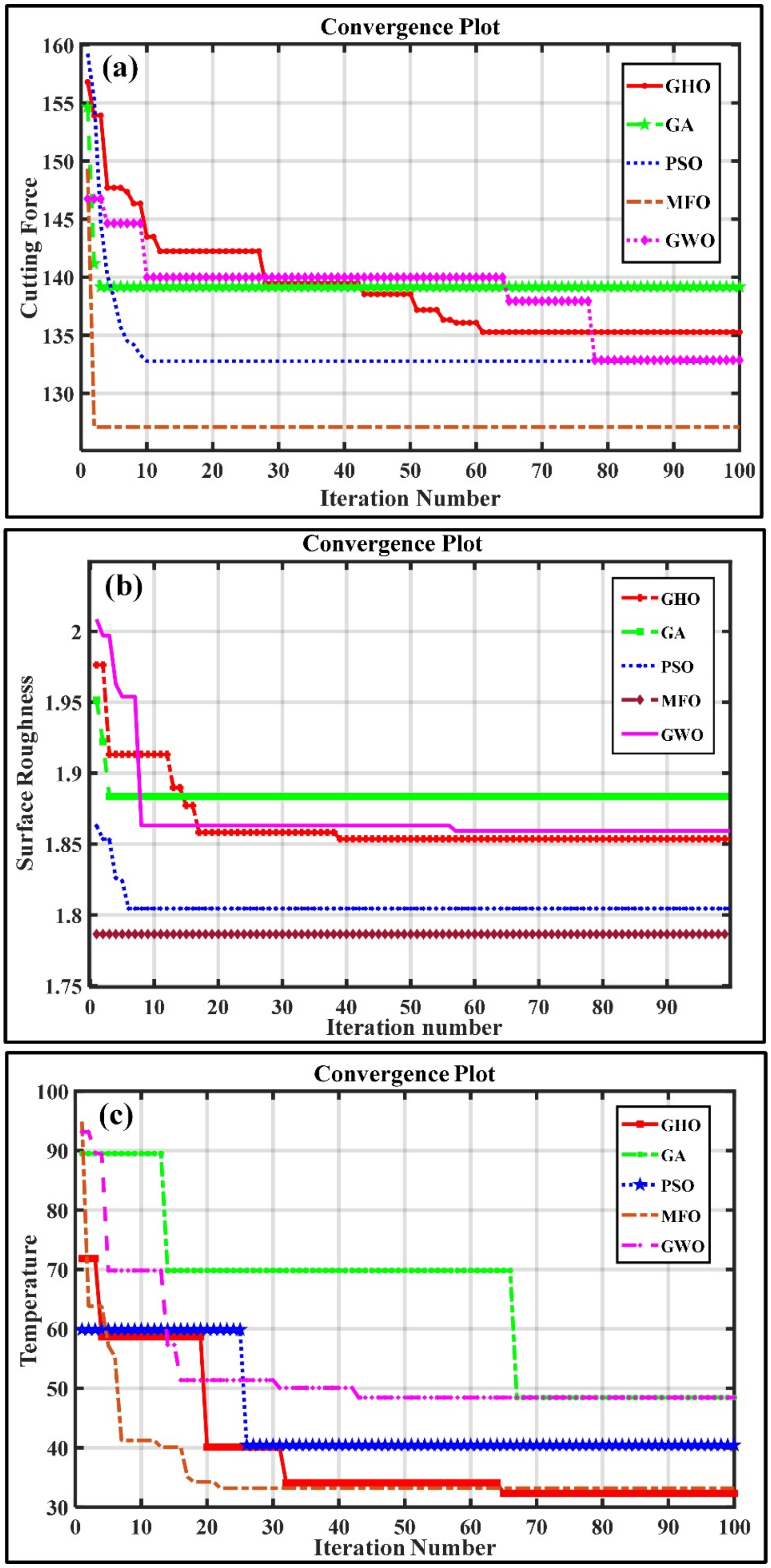

Figure 4. Convergence plot for case study 1 (**a**) Cutting Force (**b**) Surface Roughness (**c**) Cutting Temperature.

3.2. Case Study 2

In this study, the simultaneous minimization of dual machinability indices with three different combinations using evolutionary algorithms is considered. The Pareto front analyses of all the algorithms with respect to CF vs. SR, CT vs. CF, and CT vs. SR are given in Figure 5a–c, respectively. Further, the TOPSIS method is used to convert the dual machinability indices into a single objective. Hence, the global minimum value of the machinability indices is obtained using TOPSIS results (Figure 5d–f) for all the evolutionary algorithms. In addition to that, the performance of evolutionary algorithms is validated using the hypervolume indicator. From these Figure 5, it is inferred that the MFO algorithm outperformed others in all three cases. The results are presented in Table 5.

Table 5. Minimization of machinability indices based on pareto front analysis and TOPSIS method for Case study 2.

Algorithms	Machinability Indices Considered	Cutting Speed (m/min)	Feed rate (mm/rev)	Environment	Machinabilty Index Value (MI_1)	Machinabilty Index Value (MI_2)	Hyper Volume (HV)
GHO		128.00	0.050	3	127.75 N	2.26 μm	0.301
GA	CF	126.00	0.062	3	127.12 N	2.27 μm	0.302
PSO	&	128.00	0.065	3	141.07 N	2.17 μm	0.319
MFO	SR	124.00	0.060	3	136.57 N	2.20 μm	0.324
GWO		129.00	0.060	3	136.57 N	2.20 μm	0.321
GHO		53.87	0.050	3	206.31 N	42.89 °C	0.652
GA	CF	34.06	0.060	3	218.52 N	32.79 °C	0.633
PSO	&	35.06	0.062	3	218.52 N	32.79 °C	0.624
MFO	TE	35.11	0.050	3	217.98 N	31.26 °C	0.697
GWO		46.90	0.050	3	211.12 N	39.03 °C	0.657
GHO		34.32	0.052	3	2.60 μm	36.16 °C	0.391
GA	SR	34.32	0.062	3	2.60 μm	36.16 °C	0.415
PSO	&	49.38	0.058	3	2.52 μm	43.72 °C	0.416
MFO	TE	50.00	0.053	3	2.52 μm	34.06 °C	0.443
GWO		52.00	0.056	3	2.52 μm	44.06 °C	0.441

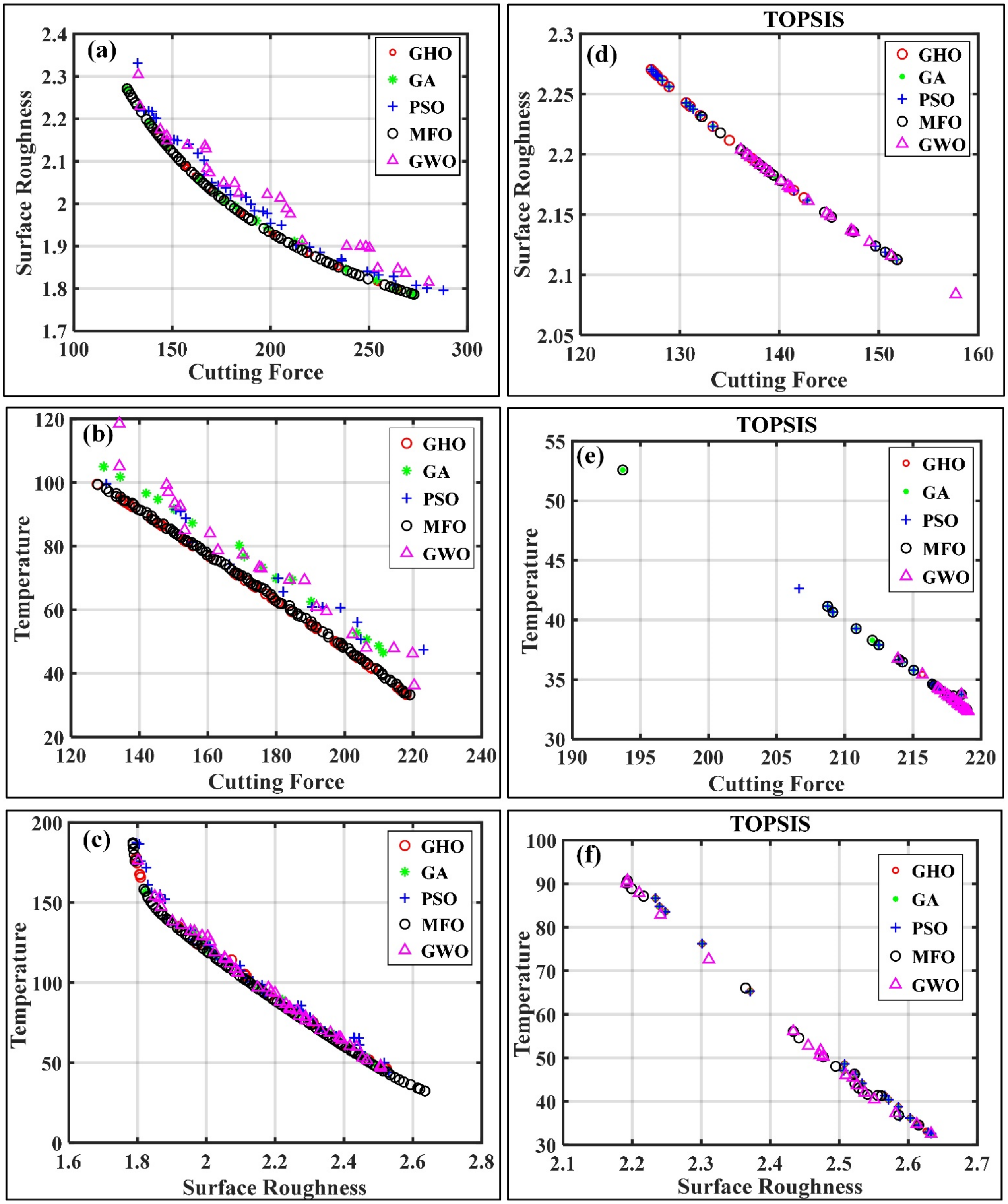

Figure 5. Pareto optimality (**a**–**c**) Multi-objective for single run (**d**–**f**) Multi-Objective for 27 runs.

The general observations are when CF increases, and SR worsens after machining; When CF increases, TE increases significantly and affects the tool life; and when TE increases, then SR decreases. Further, the LN_2 environment minimizes the CF, CT, and SR due to a fine droplet of LN_2 acting as a film barrier in the tool and workpiece interface, thus reducing chatter vibration and built-up edge formation. This is used to improve the tool life too.

3.3. Case Study 3

In this case study, the simultaneous minimization of all three machinability indices is carried out using evolutionary algorithms. As in case study 2, the TOPSIS method is used to convert all three machinability indices to a single objective. Further, the quality indicators, namely Diversity (DIV), Inverted Generational Distance (IGD), and Hyper Volume (HV), are used to opt out the best evolutionary algorithm which provides minimum values of machinability indices along with the corresponding set of turning process parameters. The algorithm, which has a higher DIV and HV value and a lower IGD value, is to be considered as the best algorithm among others. The DIV and IGD values are calculated using Equations (4) and (5), respectively. The hypervolume is calculated based on the Pareto analysis. The calculated values of quality indicators for all the algorithms are presented in Table 6.

$$DIV = \sqrt{\sum_{j=1}^{k} (f_j^{\max} - \quad f_j^{\min})^2} \tag{4}$$

$$IGD = \frac{\sqrt{\sum_{i=1}^{n} d_i^2}}{n} \tag{5}$$

$$d_i = \sqrt{\sum_{j=1}^{no} (o_{ij} - o_{bj})^2} \tag{6}$$

where,

O_{ij}—*i*th run *j*th objective value;

O_{bj}—Best *j*th objective value;

d_i—Euclidean distance.

Table 6. Minimization of machinability indices based on IGD, DIV and HV for Case study 3.

Algorithms	IGD	DIV	HV	Cutting Speed (m/min)	Feed Rate (mm/rev)	Environment	Cutting Force (N)	Surface Roughness (µm)	Temperature (°C)
GHO	7.98	233.85	0.273	71.00	0.051	3	193.36	2.44	85.25
GA	9.81	279.61	0.267	72.00	0.051	3	194.36	2.48	86.25
PSO	5.79	264.68	0.265	94.62	0.052	3	173.13	2.45	73.28
MFO	5.10	286.72	0.286	92.62	0.052	3	171.13	2.35	72.28
GWO	6.70	267.48	0.269	96.62	0.052	3	174.13	2.55	74.28

Further the statistical analyses of the quality indicators are carried out using Minitab software to study the performance and consistency of the algorithms. The normal probability plots for the quality indicators IGD, DIV, and HV are given in Figure 6a–c, respectively, and the summary reports of the same are given in Figure6d–f, respectively.

From Figure6d–f and as well as the findings (higher values of DIV and HV and Lower value of IGD) from Table 5, it is concluded that the MFO algorithm outperformed others.

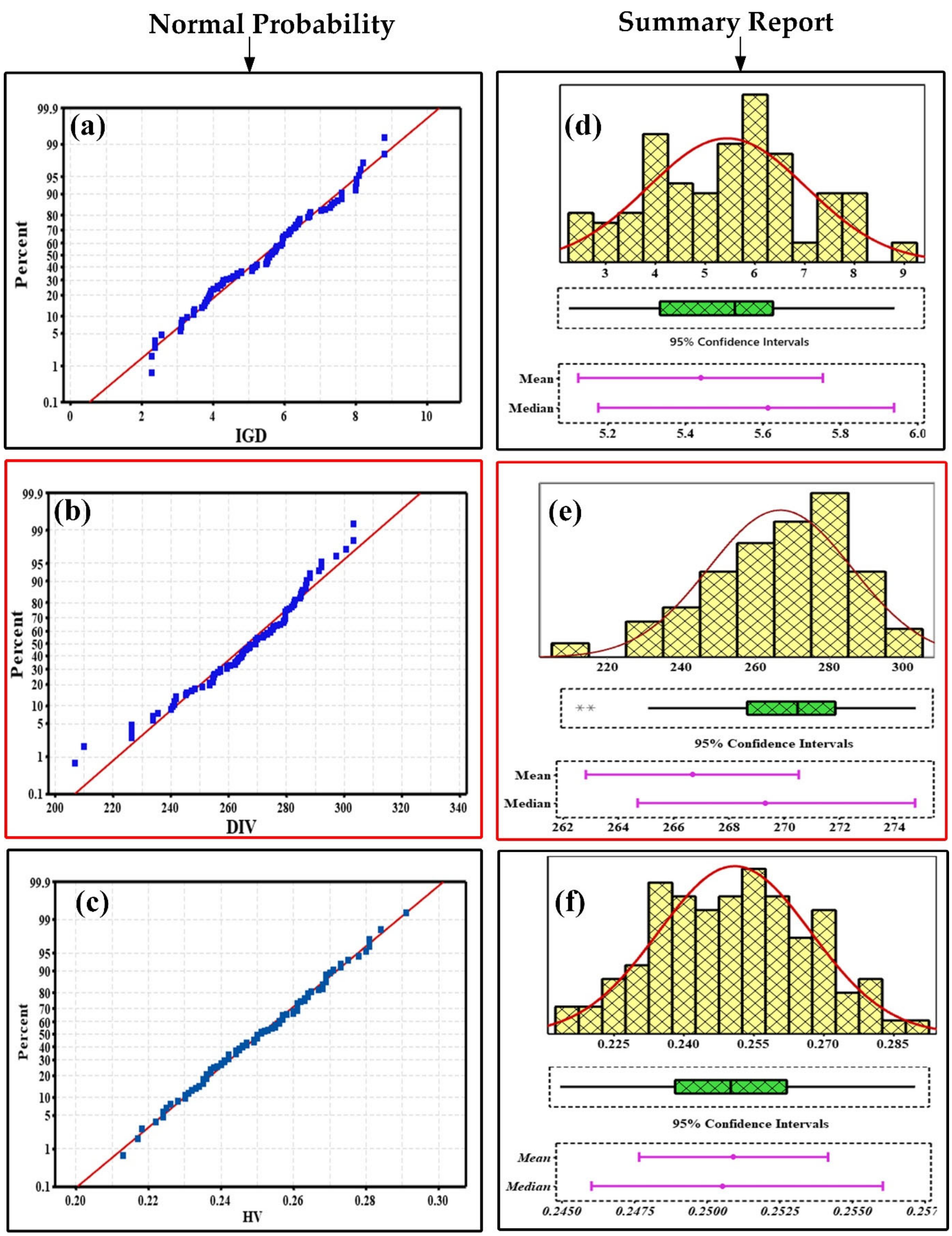

Figure 6. (**a–c**) Normal Probability plot (**d–f**) summary report.

The reasons for the better performance of MFO compared with other algorithms are explained here. The GA became gradually a dominant optimization technique compared to deterministic approaches mainly due to the higher probability of local solutions avoidance. However, the main drawback of GA was the stochastic nature of this algorithm which resulted in finding different solutions in every run. Despite the relatively high convergence rate of PSO, it has the drawback of premature convergence to local optimal and ineffectiveness in exploring the whole search space. Similarly, the original version of the GWO algorithm has the drawbacks of low solving accuracy, bad local searching ability, and slow convergence rate. Similarly, the disadvantage of GHO was being easy to fall into the local optimum which prevented the search process from finding a better solution. On the other hand, MFO is able to locate the local and global optimal solutions accurately with less computational time [43].

4. Conclusions

The purpose of this study was to minimize machinability indices CF, SR, and CT while performing the turning of Hastelloy X. Three levels of turning process parameters namely cutting speed (v_c), feed rate f, and machining environment were considered for performing the experiments under L_{27} orthogonal array basis. Further, the MFO algorithm was used to identify the optimal set of turning process parameters to minimize the machinability indices individually and simultaneously. Three case studies were carried out for this purpose. The conclusion drawn from these case studies is given below.

1. From the case study 1 (minimization of machinability indices individually), as compared to other algorithms such as GHO, GA, PSO, and GWO, the MFO algorithm yielded the minimum values of CF = 127.1 N, SR = 1.78μm, and CT = 33.19 ºC for the optimal set of turning process parameters such as v_c =124m/min, f = 0.05 mm/rev, and cryogenic environment. The range of reduction in CF, SR, and CT values based on the MFO algorithm was 4-8 %, 1-23%, and 3-57%, respectively, compared with other algorithms.
2. The simultaneous minimization of dual machinability indices with three combinations were performed using the MFO algorithm in case study 2. The results were compared with the results obtained from other algorithms. Based on the hypervolume indicator identified from the Pareto analyses, again the MFO outperformed others, and the corresponding optimal set of input parameters were identified.
3. In case study 3, the simultaneous minimization of all three machinability indices was carried out using the MFO algorithm. The performance of MFO algorithm was compared with other algorithms using the quality indicators namely Diversity, Inverted Generational Distance, and Hyper Volume. From the analyses, the best results were obtained as CF = 171.13 N, SR = 2.35 μm and CT = 72.28 ºC form the MFO algorithm for the inputs of v_c = 93 m/min, f = 0.05 mm/rev and cryogenic environment.

Based on the results of all three case studies, the MFO algorithm effectively predicted the optimal set of turning process parameters in view of minimizing the machinability indices individually and simultaneously when compared with other algorithms. Further, the other machinability indices such as tool life and machining cost will also be considered in addition to the existing indices as the future work.

Author Contributions: Conceptualization, V.S.; Methodology, V.S., J.S. and Y.N.; Experimental design, V.S. and J.S.; Experimental setup, V.S.; Measurements, V.S., S.K.M. and Y.N.; Investigation, L.N., S.K.M. and Y.N.; Resources, L.N., S.K.M. and Y.N.; Visualization, V.S., L.N., S.K.M. and S.S.; Writing—Original Draft Preparation, V.S., J.S., L.N., S.K.M., Y.N., S.S., E.A.N., J.P.D. and H.M.A.M.H.; Writing—Review & Editing, V.S., J.S., L.N., S.K.M., Y.N. and S.S.; Supervision, J.S. and V.S.; Project administration, V.S. and J.S.; Funding acquisition, J.S. and S.S. All authors have read and agreed to the published version of the manuscript.

Funding: This research has received funding from King Saud University through Researchers Supporting Project number (RSP-2021/164), King Saud University, Riyadh, Saudi Arabia. Moreover, this is part of the project was financially supported by Fundamental Research Fund of Shandong

University under the funding code No. 2019HW040. the Future for Young Scholars of Shandong University, China under the funding code No. 31360082064026.

Institutional Review Board Statement: Not applicable.

Informed Consent Statement: Not applicable.

Data Availability Statement: Not applicable.

Acknowledgments: The authors extend their appreciation to King Saud University for funding this work through Researchers Supporting Project number (RSP-2021/164), King Saud University, Riyadh, Saudi Arabia.

Conflicts of Interest: The authors declare no conflict of interest.

References

1. Sivalingam, V.; Zhuoliang, Z.; Jie, S.; Baskaran, S.; Yuvaraj, N.; Gupta, M.K.; Aqib, M.K. Use of Atomized Spray Cutting Fluid Technique for the Turning of a Nickel Base Superalloy. *Mater. Manuf. Process.* **2021**, *36*, 373–380.
2. METODO. Optimization of the turning parameters for the cutting forces in the Hastelloy X superalloy based on the Taguchi method. *Mater. Tehnol.* **2014**, *48*, 249–254.
3. Kadirgama, K.; Abou-El-Hossein, K.A; Mohammad, B.; Al-Ani, H.; Noor, M. Cutting force prediction model by FEA and RSM when machining Hastelloy C-22HS with 90 holder. **2008**, *67*, 421–427. DOI: http://nopr.niscair.res.in/handle/123456789/1370
4. Kadirgama, K.; Abou-El-Hossein, K.; Noor, M.; Sharma, K.; Mohammad, B. Tool life and wear mechanism when machining Hastelloy C-22HS. *Wear* **2011**, *270*, 258–268.
5. Sofuoğlu, M.A.; Çakır, F.H.; Gürgen, S.; Orak, S.; Kuşhan, M.C. Experimental investigation of machining characteristics and chatter stability for Hastelloy-X with ultrasonic and hot turning. *Int. J. Adv. Manuf. Technol.* **2018**, *95*, 83–97.
6. Dhananchezian, M. Study the machinability characteristics of Nicked based Hastelloy C-276 under cryogenic cooling. *Measurement* **2019**, *136*, 694–702.
7. Kesavan, J.; Senthilkumar, V.; Dinesh, S. Experimental and numerical investigations on machining of Hastelloy C276 under cryogenic condition. *Mater. Today Proc.* **2020**, *27*, 2441–2444.
8. Dhananchezian, M.; Rajkumar, K. Comparative study of cutting insert wear and roughness parameter (Ra) while turning Nimonic 90 and hastelloy C-276 by coated carbide inserts. *Mater. Today Proc.* **2020**, *22*, 1409–1416.
9. Oschelski, T.B.; Urasato, W.T.; Amorim, H.J.; Souza, A.J. Effect of cutting conditions on surface roughness in finish turning Hastelloy® X superalloy. *Mater. Today Proc.* **2021**, *44 (part 1)*, 532–537.
10. Venkatesan, K.; Devendiran, S.; Nishanth Purusotham, K.; Praveen, V.S. Study of machinability performance of Hastelloy-X for nanofluids, dry with coated tools. *Mater. Manuf. Process.* **2020**, *35*, 751–761.
11. Sivalingam, V.; Zan, Z.; Sun, J.; Selvam, B.; Gupta, M.K.; Jamil, M.; Mia, M. Wear behaviour of whisker-reinforced ceramic tools in the turning of Inconel 718 assisted by an atomized spray of solid lubricants. *Tribol. Int.* **2020**, *148*, 106235.
12. Zhao, Y.; Li, J.; Guo, K.; Sivalingam, V.; Sun, J. Study on chip formation characteristics in turning NiTi shape memory alloys. *J. Manuf. Process.* **2020**, *58*, 787–795.
13. Chetan; Gosh, S.; Rao, P.V. Environment friendly machining of Ni–Cr–Co based super alloy using different sustainable techniques. *Mater. Manuf. Process.* **2016**, *31*, 852–859.
14. Iturbe, A.; Hormaetxe, E.; Garay, A.; Arrazola, P. Surface integrity analysis when machining Inconel 718 with conventional and cryogenic cooling. *Procedia CIRP* **2016**, *45*, 67–70.
15. Sivaiah, P.; Chakradhar, D. Influence of cryogenic coolant on turning performance characteristics: A comparison with wet machining. *Mater. Manuf. Process.* **2017**, *32*, 1475–1485.
16. Tebaldo, V.; di Confiengo, G.G.; Faga, M.G. Sustainability in machining: "Eco-friendly" turning of Inconel 718. Surface characterisation and economic analysis. *J. Clean. Prod.* **2017**, *140*, 1567–1577.
17. Shokrani, A.; Al-Samarrai, I.; Newman, S.T. Hybrid cryogenic MQL for improving tool life in machining of Ti-6Al-4V titanium alloy. *J. Manuf. Process.* **2019**, *43*, 229–243.
18. Mehta, A.; Hemakumar, S.; Patil, A.; Khandke, S.; Kuppan, P.; Oyyaravelu, R.; Balan, A. Influence of sustainable cutting environments on cutting forces, surface roughness and tool wear in turning of Inconel 718. *Mater. Today Proc.* **2018**, *5*, 6746–6754.
19. Khalilpourazari, S.; Khalilpourazary, S. Optimization of production time in the multi-pass milling process via a Robust Grey Wolf Optimizer. *Neural Comput. Appl.* **2018**, *29*, 1321–1336.
20. Khalilpourazari, S.; Khalilpourazary, S. A lexicographic weighted Tchebycheff approach for multi-constrained multi-objective optimization of the surface grinding process. *Eng. Optim.* **2017**, *49*, 878–895.
21. Khalilpourazari, S.; Khalilpourazary, S. A Robust Stochastic Fractal Search approach for optimization of the surface grinding process. *Swarm Evol. Comput.* **2018**, *38*, 173–186.
22. Rao, R.V.; Rai, D.P.; Balic, J. Multi-objective optimization of abrasive waterjet machining process using Jaya algorithm and PROMETHEE Method. *J. Intell. Manuf.* **2019**, *30*, 2101–2127.

23. Rao, R.V.; Rai, D.P.; Balic, J. A multi-objective algorithm for optimization of modern machining processes. *Eng. Appl. Artif. Intell.* **2017**, *61*, 103–125.
24. Khalilpourazari, S.; Khalilpourazary, S. Optimization of time, cost and surface roughness in grinding process using a robust multi-objective dragonfly algorithm. *Neural Comput. Appl.* **2020**, *32*, 3987–3998.
25. Khalilpourazari, S.; Khalilpourazary, S. SCWOA: An efficient hybrid algorithm for parameter optimization of multi-pass milling process. *J. Ind. Prod. Eng.* **2018**, *35*, 135–147.
26. Almeida, J.H.S., Jr.; St-Pierre, L.; Wang, Z.; Ribeiro, M.L.; Tita, V.; Amico, S.C.; Castro, S.G. Design, modeling, optimization, manufacturing and testing of variable-angle filament-wound cylinders. *Compos. Part B Eng.* **2021**, *225*, 109224.
27. Wang, Z.; Almeida, J.H.S., Jr.; St-Pierre, L.; Wang, Z.; Castro, S.G. Reliability-based buckling optimization with an accelerated Kriging metamodel for filament-wound variable angle tow composite cylinders. *Compos. Struct.* **2020**, *254*, 112821.
28. Almeida, J.H.S., Jr.; Ribeiro, M.L.; Tita, V.; Amico, S.C. Stacking sequence optimization in composite tubes under internal pressure based on genetic algorithm accounting for progressive damage. *Compos. Struct.* **2017**, *178*, 20–26.
29. Sridhar, R.; Subramani, C.; Pathy, S. A grasshopper optimization algorithm aided maximum power point tracking for partially shaded photovoltaic systems. *Comput. Electr. Eng.* **2021**, *92*, 107124.
30. Purushothaman, R.; Rajagopalan, S.; Dhandapani, G. Hybridizing Gray Wolf Optimization (GWO) with Grasshopper Optimization Algorithm (GOA) for text feature selection and clustering. *Appl. Soft Comput.* **2020**, *96*, 106651.
31. Steczek, M.; Jefimowski, W.; Szeląg, A. Application of Grasshopper Optimization Algorithm for Selective Harmonics Elimination in Low-Frequency Voltage Source Inverter. *Energies* **2020**, *13*, 6426.
32. Sangwan, K.S.; Kant, G. Optimization of machining parameters for improving energy efficiency using integrated response surface methodology and genetic algorithm approach. *Procedia CIRP* **2017**, *61*, 517–522.
33. Hazir, E.; Ozcan, T. Response surface methodology integrated with desirability function and genetic algorithm approach for the optimization of CNC machining parameters. *Arab. J. Sci. Eng.* **2019**, *44*, 2795–2809.
34. Almeida, J.H.S., Jr.; Bittrich, L.; Nomura, T.; Spickenheuer, A. Cross-section optimization of topologically-optimized variable-axial anisotropic composite structures. *Compos. Struct.* **2019**, *225*, 111150.
35. Johari, N.F.; Zain, A.M.; Mustaffa, N.H.; Udin, A. Machining parameters optimization using hybrid firefly algorithm and particle swarm optimization. In *Journal of Physics: Conference Series*; IOP Publishing: Tokyo, Japan, 2017; Volume 892, p. 012005.
36. Lmalghan, R.; Rao, K.; ArunKumar, S.; Rao, S.S.; Herbert, M.A. Machining parameters optimization of AA6061 using response surface methodology and particle swarm optimization. *Int. J. Precis. Eng. Manuf.* **2018**, *19*, 695–704.
37. Tamilarasan, A.; Rajmohan, T.; Ashwinkumar, K.; Dinesh, B.; Praveenkumar, M.; Reddy, R.D.; Kiran, K.S.; Elangumaran, R.; Krishnamoorthi, S. Hybrid WCMFO algorithm for the optimization of AWJ process parameters. In *IOP Conference Series: Materials Science and Engineering*; IOP Publishing: Tokyo, Japan, 2020; Volume 954; p. 012041.
38. Kamaruzaman, A.F.; Zain, A.M.; Alwee, R.; Yusof, N.M.; Najarian, F. Optimization of Surface Roughness in Deep Hole Drilling using Moth-Flame Optimization. *ELEKTRIKA J. Electr. Eng.* **2019**, *18*, 62–68.
39. Fountas, N.; Koutsomichalis, A.; Kechagias, J.; Vaxevanidis, N. Multi-response optimization of CuZn39Pb3 brass alloy turning by implementing Grey Wolf algorithm. *Frat. Ed Integrità Strutt.* **2019**, *13*, 584–594.
40. Sibalija, T.V.; Kumar, S.; Patel, G.M. A soft computing-based study on WEDM optimization in processing Inconel 625. *Neural Comput. Appl.* **2021**, *1–22*.
41. Sekulic, M.; Pejic, V.; Brezocnik, M.; Gostimirović, M.; Hadzistevic, M. Prediction of surface roughness in the ball-end milling process using response surface methodology, genetic algorithms, and grey wolf optimizer algorithm. *Adv. Prod. Eng. Manag.* **2018**, *13*, 18–30.
42. Dhananchezian, M.; Rajkumar, K. Cryogenic turning of Hastelloy C-22. *Mater. Today Proc.* **2020**, *22*, 3075–3081.
43. Yang, Z.; Shi, K.; Wu, A.; Qiu, M.; Hu, Y. A hybird method based on particle swarm optimization and moth-flame optimization. In Proceedings of the 11th International Conference on Intelligent Human-Machine Systems and Cybernetics (IHMSC), Hangzhou, China, 24–25 August 2019; Volume 2, pp. 207–210.